THE JOURNAL OF PHYSICAL CHEMISTRY A

Article

pubs.acs.org/JPCA

Photophysics of Platinum Tetrayne Oligomers: Delocalization of Triplet Exciton

Yongjun Li,[†] Russell W. Winkel,[†] Nancy Weisbach,[‡] John A. Gladysz,*[,‡] and Kirk S. Schanze*[,†]

[†]Department of Chemistry, University of Florida, P.O. Box 117200, Gainesville, Florida 32611, United States

[‡]Chemistry Department, Texas A&M University, P.O. Box 30012, College Station, Texas 77842, United States

Supporting Information

ABSTRACT: A series of platinum tetrayne oligomers, *all-trans*-Cl−Pt(P_2)−[(C≡C)$_4$−Pt(P_2)]$_n$−Cl, where P = tri(*p*-tolyl)phosphine and n = 1−3, was subjected to a detailed photophysical investigation. The photoluminescence of each oligomer at low temperature (T < 140 K) in a 2-methyltetrahydrofuran (Me-THF) glass features an intense and narrow 0−0 phosphorescence band accompanied by a vibronic progression of sub-bands separated by ca. 2100 cm^{-1}. The emission arises from a $^3\pi,\pi^*$ triplet state concentrated on the (C≡C)$_4$ carbon chain and the vibronic progression originates from coupling of the excitation to the ν (C≡C) stretch. All of the experimental data including ambient temperature absorption, low-temperature photoluminescence, and ambient temperature transient absorption spectroscopy provide clear evidence that the triplet state is localized on a chromophore consisting of approximately two −[(C≡C)$_4$−Pt(P_2)]− repeat units. Density functional theory calculations support the hypothesis that the triplet−triplet absorption arises from transitions that are delocalized over two repeat units.

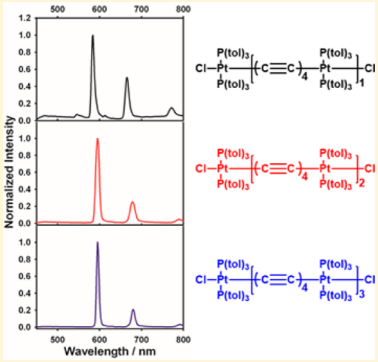

INTRODUCTION

Organic and organometallic oligomers that feature extended sp carbon chains, for example, R−(C≡C)$_n$−R and L$_y$M−(C≡C)$_n$−ML$_y$ have attracted recent interest due to their potential application in optical and optoelectronic devices.[1−10] Oligoynes feature rigid rod-like structures and extended π-electron delocalization, which makes them attractive building blocks for the construction of linear carbon-rich materials that may possess potential applications as molecular electronic wires for studying exciton or charge transport on the nanoscale.[11,12]

Transition metals, such as rhenium, iron, ruthenium, platinum, manganese, and gold, have been incorporated as end-groups on the oligoyne chains to increase the stability of linear carbon chain compounds.[3,6,7,13−16] Most studies of these transition-metal-containing carbon chain compounds have focused on synthesis, structural properties, and optical absorption spectroscopy. However, an important feature of these compounds is that their triplet excited states are produced in relatively high yield due to the strong spin−orbit coupling induced by the transition metals. There are only a few reports concerning this aspect.[8,15] Yam and coworkers described a spectroscopic study of a series of platinum(II)-terpyridyl-capped carbon chains.[15] They found that low-temperature photoluminescence of these complexes features phosphorescence emission originating from the carbon chain $^3(\pi,\pi^*)$ state with a vibronic progression spacing of ca. 2052 cm^{-1}. Che and coworkers investigated a series of gold end-capped carbon chain compounds.[8] Their spectroscopic results indicate that the lowest-energy electronic excited states are dominated by the acetylenic $^3(\pi,\pi^*)$ transition and a well-defined vibronic progression with a spacing of ca. 2000 cm^{-1} that corresponds to the ν (C≡C) stretch in the $^3(\pi \rightarrow \pi^*)$ excited state.

We recently reported a photophysical study of a series of platinum end-capped polyyne oligomers that feature increasing sp carbon chain length (Scheme 1).[17] The results of this study indicated that the low-temperature photoluminescence spectra exhibit moderately efficient phosphorescence appearing as a series of narrow vibronic bands separated by ca. 2100 cm^{-1}. The emission originates from the sp carbon chain $^3(\pi,\pi^*)$ transition, and the vibronic progression arises from coupling of the excitation to the ν(C≡C) stretch. With increasing sp carbon chain length, the 0−0 energy of the phosphorescence decreases across the series. Moreover, a quantitative energy gap

Scheme 1. Platinum End-Capped Polyynes Pt$_2$(C$_2$)$_n$ Studied by Farley et al.[17]

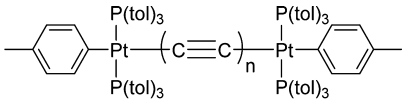

Pt$_2$(C$_2$)$_n$

n = 3, 4, 5, 6

tol = p-tolyl

Special Issue: Current Topics in Photochemistry

Received: March 1, 2014
Revised: May 9, 2014

law correlation was revealed through an analysis of the triplet nonradiative decay rates in the series.

While there have been a number of studies of transition-metal end-capped linear carbon chain molecules, little work has been done on metal−carbon chain alternant oligomers, for example, M−[(C≡C)$_n$−M]$_m$. In particular, a photophysical study of this type of structure with $n > 2$ and $m > 1$ has not been previously reported. However, investigation of this type of oligomer is very important because it provides a unique platform to study triplet exciton delocalization, providing insight that could extend to exciton transport in "molecular wires".[11,12,18] To allow the photophysical study of this type of metal-bridged oligomeric carbon chains, one of our groups synthesized and structurally characterized a series of platinum-containing tetrayne oligomers of the type *all-trans*−Cl-Pt(P$_2$)−[(C≡C)$_4$-Pt(P$_2$)]$_n$−Cl, where P represents a phosphine ligand and n = 1−3.[19]

Here we report a detailed study of the photophysics of the series of platinum tetrayne oligomers, $(\mathbf{PtC_8})_n$ (n = 1, 2, 3; Scheme 2). These systems feature a carbon chain of constant

Scheme 2. Platinum Tetrayne Oligomers

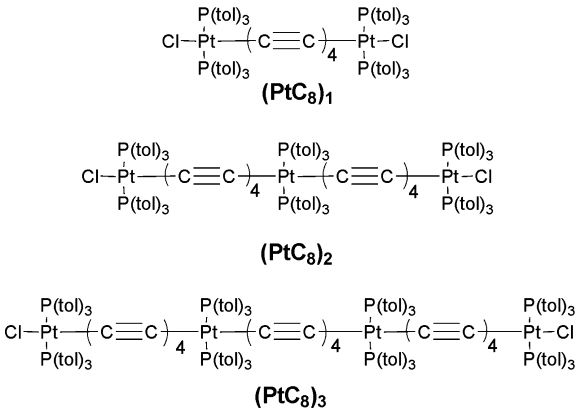

length (C_8) in oligomeric structures linked by intervening Pt(P(tol)$_3$)$_2$ units. The properties of the triplet excited states in the oligomers were probed by steady-state and time-resolved luminescence spectroscopy and by transient absorption spectroscopy. The key objective of the work is to discover whether the triplet exciton state is delocalized in the longer chain oligomer sections and how the delocalization influences the energy and dynamics of the excited state. The results support a model in which the triplet exciton is delocalized over at least two C_8 chains, as evidenced by the effect of oligomer length on the triplet spectroscopy and dynamics. Interestingly, the triplet−triplet absorption varies noticeably across the entire series, suggesting that the optical transition accesses states (T_2 or higher) that are more delocalized than the lowest triplet state.

■ EXPERIMENTAL SECTION

Photophysical Measurements. Steady-state absorption spectra were recorded on a Varian Cary 100 dual-beam spectrophotometer. Corrected steady-state emission measurements were conducted on a SPEX F-112 fluorescence spectrometer. Samples were degassed by argon purging for 30 min, and concentrations were adjusted such that the solutions were optically dilute (A_{max}< 0.20). Low-temperature emission measurements were conducted in 1 cm diameter borosilicate glass tubes in a liquid-nitrogen-cooled Oxford Instruments DN-1704 optical cryostat connected to an Omega CYC3200 autotuning temperature controller. Samples were degassed by three consecutive freeze−pump−thaw cycles on a high-vacuum (10^{-5} Torr) line.

Photoluminescence quantum yields were determined by relative actinometry. Ru(bpy)$_3^{2+}$ (Φ_F = 0.0379 in air-saturated H_2O) was used as the actinometer. Time-resolved emission measurements were conducted on a previously described home-built apparatus.[17] Optically dilute solutions were used.

Transient absorption measurements were carried out on a home-built apparatus consisting of a Continuum Surelite series Nd:YAG laser as the excitation source (λ = 355 nm, 10 ns fwhm). Typical excitation energies were 5 mJ/pulse. The source for monitoring optical transients was a Hamamatsu Super-Quiet series xenon flashlamp, and the monitoring light was detected by a Princeton Instruments PI-MAX intensified CCD camera detector coupled to an Acton SpectroPro 150 spectrograph. Samples were contained in a cell with a total volume of 10 mL, and the contents were continuously circulated through the pump−probe region of the cell. Solutions were degassed by argon purging for 30 min. Sample concentrations were adjusted so that $A_{355} \approx 0.8$. Principal component transient absorption difference spectra were obtained by global analysis of the time-resolved absorption data using Specfit32 software (Spectrum Software Associates, distributed by TgK Scientific, http://www.hi-techsci.com/products/specfitglobalanalysis/).[20]

Photoluminescence Spectral Fitting. The spectral fitting was carried out according to the method described by Farley.[17]

Density Functional Theory Calculations. All calculations were carried out using DFT as implemented in Gaussian 09 rev. C.01 (Gaussian, Inc., Wallingford, CT, 2009). Geometries were optimized using the B3LYP functional along with the 6-31G(d) basis set for C, H, and Cl, the 6-31+G(d) basis set for P, and the SDD basis set for Pt. To minimize computational cost, we replaced Ptol$_3$ moieties with PMe$_3$ (Me: methyl). These models are designated by the addition of a prime (′) to their name, and thus the model for $(\mathbf{PtC_8})_1$ is termed as $(\mathbf{PtC_8})_1'$. All singlet optimizations were started from idealized geometries and run without symmetry constraints. Triplet optimizations were initiated from the optimized singlet geometry and used the unrestricted B3LYP functional. All optimized structures were characterized by vibrational frequency calculations and were shown to be minima by the absence of imaginary frequencies. Time-dependent DFT calculations were performed for all optimized structures at the same level of theory with the same basis sets. Structures were visualized using Chemcraft version 1.7 (http://www.chemcraftprog.com, 2012).

■ RESULTS AND DISCUSSION

UV−visible Absorption Spectroscopy. Absorption spectra for the series of compounds $(\mathbf{PtC_8})_n$ were reported previously in CH_2Cl_2 solution, including molar extinction coefficients. (The peak molar absorptivity values vary from 70 000 to 250 000 $M^{-1}cm^{-1}$, increasing with length.[19]) For completeness in the course of the present study, we recorded the spectra in 2-methyltetrahydrofuran (Me-THF) solutions, and they are shown in a normalized format in Figure 1. All three oligomers feature two primary electronic transitions, each of which appears as a manifold of vibronic bands. In general, the high-energy transition occurs between 300 and 380 nm and the low-energy transition occurs between 380 and 450 nm.

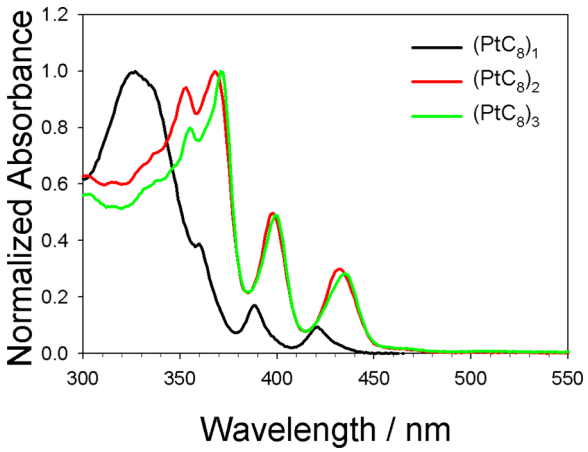

Figure 1. Absorption spectra of $(\mathbf{PtC_8})_n$ complexes in Me-THF solution.

Both transitions red-shift with increasing oligomer length. The red-shift from $(\mathbf{PtC_8})_1$ to $(\mathbf{PtC_8})_2$ is evident (~10 nm, 650 cm^{-1}). However, the red-shift is small from $(\mathbf{PtC_8})_2$ to $(\mathbf{PtC_8})_3$, indicating that the effective conjugation length for the optical transition is two PtC_8 repeat units. The low-energy transition is weak, whereas the higher energy transition is relatively more intense. For $(\mathbf{PtC_8})_2$ and $(\mathbf{PtC_8})_3$, a well-defined vibronic progression appears in both transitions. For $(\mathbf{PtC_8})_1$, the high-energy transition features a broad absorption band along with a weak vibronic shoulder. By comparison with previous studies,[17,21] the low-energy band originates from the π,π^* transition that has its basis in the π-system that interacts with the Pt(II) end groups (via dπ−pπ overlap), whereas the high-energy band originates from the π,π^* transition that originates on the $-(C{\equiv}C)_4-$ π-system that is orthogonal to the Pt dπ orbitals. The molar extinction coefficients of $(\mathbf{PtC_8})_1$ to $(\mathbf{PtC_8})_3$ are proportional to the number of tetrayne units.[19]

Phosphorescence Emission Spectroscopy. Photoluminescence spectra for the complexes $(\mathbf{PtC_8})_n$ were recorded in deoxygenated Me-THF solution at temperatures ranging from 300 to 80 K. On the basis of the observed lifetimes (several microseconds, vide infra) the photoluminescence is assigned to the triplet state (phosphorescence). (An emission band assignable to fluorescence is not seen in the spectra. This is consistent with a relatively large intersystem crossing rate, $k_{isc} \approx 10^{11}$ to 10^{12} s^{-1}). Figure 2 shows the phosphorescence spectra at 100 K in the Me-THF solvent glass. Several features can be seen from the spectra. First, all of the complexes exhibit an intense and narrow 0−0 emission band followed by two vibronic progression sub-bands. The 0−0 bands are assigned to phosphorescence from $^3\pi,\pi^*$ excited states, and the vibronic sub-bands in each spectrum arise due to coupling of the triplet excitation to the $\nu(C{\equiv}C)$ stretching mode of the carbon chain. Second, the 0−0 phosphorescence band is red-shifted ca. 10 nm (290 cm^{-1}) going from $(\mathbf{PtC_8})_1$ (λ_{em} = 585 nm) to $(\mathbf{PtC_8})_2$ (λ_{em} = 595 nm), whereas there is no shift from $(\mathbf{PtC_8})_2$ to $(\mathbf{PtC_8})_3$. This indicates that the triplet exciton is delocalized over two repeat units, with possible increased delocalization into a third segment in the compound $(\mathbf{PtC_8})_3$. Third, the ratio of the intensity of 0−1 to 0−0 bands (I_{0-1}/I_{0-0}) decreases with increasing chain length. Interestingly, the ratio drops from 0.5 to 0.25 between $(\mathbf{PtC_8})_1$ and $(\mathbf{PtC_8})_2$ but it is then approximately the same for $(\mathbf{PtC_8})_2$ and $(\mathbf{PtC_8})_3$. This observation is consistent with the trends in the absorption

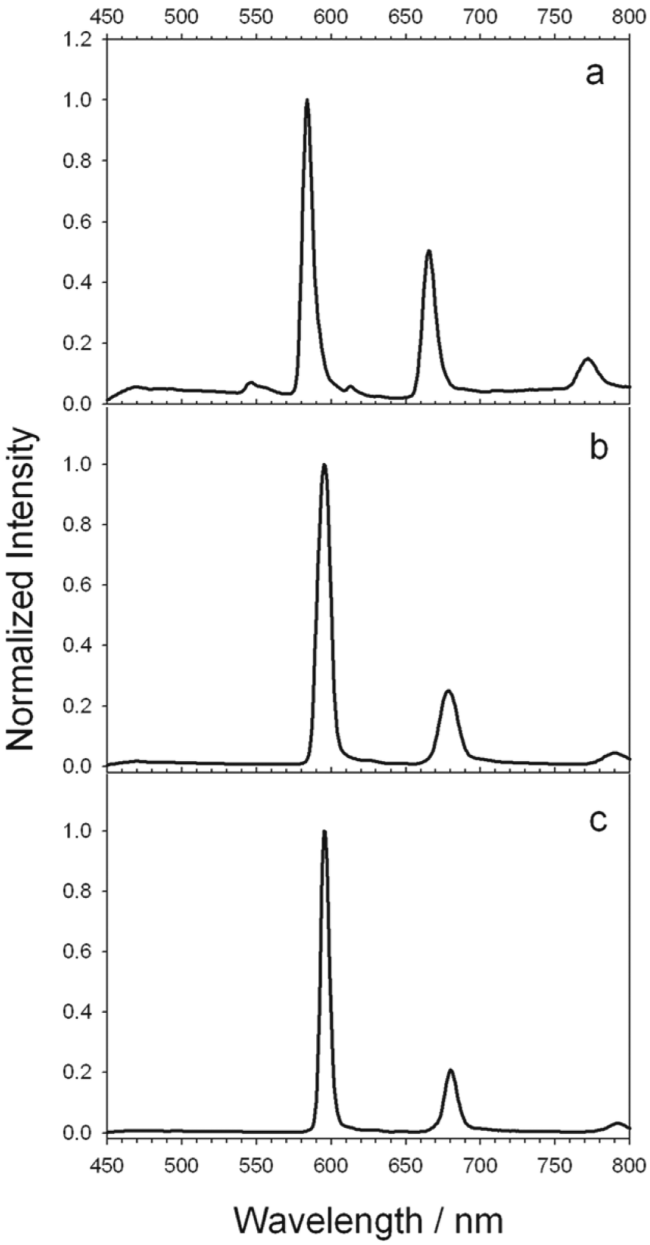

Figure 2. Photoluminescence spectra of $(\mathbf{PtC_8})_n$ in deoxygenated Me-THF solvent glass at 100 K. (a) $(\mathbf{PtC_8})_1$, λ_{ex} = 327 nm. (b) $(\mathbf{PtC_8})_2$, λ_{ex} = 368 nm. (c) $(\mathbf{PtC_8})_3$, λ_{ex} = 371 nm.

and phosphorescence maxima, which imply that the triplet state is delocalized across two repeat units. The vibronic sub-bands separated by ca. 2100 cm^{-1} reflect the dominant vibrational progression in the phosphorescence. However, a weak shoulder on the red side of the 0−0 band in $(\mathbf{PtC_8})_1$ is evident and also can be seen in other oligomers. This is likely due to the weak coupling of the excitation to carbon-chain bending modes, consistent with the similar observation on the platinum end-capped oligomers.[17]

With increasing temperature above 100 K, the phosphorescence intensity steadily decreases. However, the spectra red-shift only slightly (ca. 4 nm, 80 → 300 K), and the band shape does not change. The temperature-dependent spectra of $(\mathbf{PtC_8})_2$ are shown in Figure 3, and the spectra of the other two complexes follow a similar trend. The phosphorescence quantum yields measured at room temperature are in the range

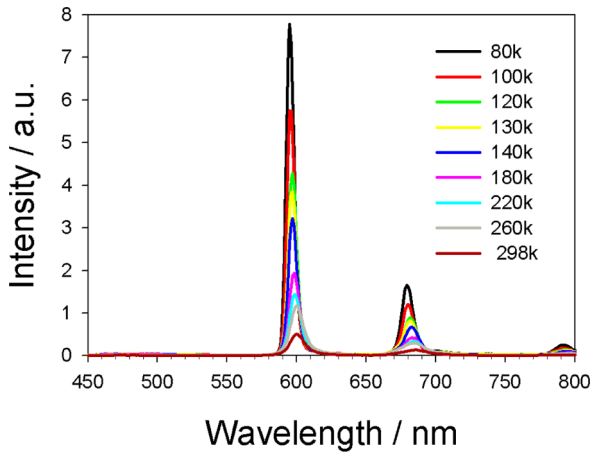

Figure 3. Variable-temperature photoluminescence spectra of $(\mathbf{PtC_8})_2$ in deoxygenated Me-THF, λ_{ex} = 368 nm. Spectra were obtained under identical conditions, so the relative intensities reflect the temperature dependence in the emission quantum yield.

of 1−4 × 10^{-3}, increasing with chain length. (The quantum yield values are tabulated along with other photophysical parameters described below in Table 2.) Excitation spectra were also obtained for all of the complexes monitored at 0−0 emission peak at 100 K in Me-THF glass. (See Figure S-1 in the Supporting Information.) The spectra are similar to the absorption spectra, except that the bands in the excitation spectra are better resolved, likely due to the frozen glass matrix.

As previously noted, the photoluminescence spectra of all three complexes appear as a narrow 0−0 band with two vibronic sub-bands separated by ~2100 cm^{-1}. The vibronic progression derives from the stretching mode of the $(C{\equiv}C)_4$ chains. To gain further insight into the nature of the luminescent triplet state, the photoluminescence spectra of $(\mathbf{PtC_8})_1$, $(\mathbf{PtC_8})_2$, and $(\mathbf{PtC_8})_3$ at 100 K were fitted utilizing methods previously described[17,22] by the single-mode Franck−Condon expression shown in eq 1.

$$I(\bar{\nu}) = \sum_{\nu_m=0}^{5} \left\{ \left(\frac{E_{00} - \nu_m \hbar\omega_m}{E_{00}} \right)^3 \frac{(S_m)^{\nu_m}}{\nu_m!} \exp\left[-4 \ln 2 \left(\frac{\bar{\nu} - E_{00} + \nu_m \hbar\omega_m}{\Delta\bar{\nu}_{0,1/2}} \right)^2 \right] \right\} \quad (1)$$

Here $I(\nu)$ is the relative emission intensity at energy ν, E_{00} is the energy of the 0−0 transition, ν_m is the quantum number of the average medium-frequency vibrational mode, $\hbar\omega_m$ is the average medium-frequency acceptor modes coupled to the triplet-excited-state to ground-state transition, S_m is the Huang−Rhys factor, and $\Delta\nu_{0,1/2}$ is the half-width of the individual vibronic bands. The experimental emission spectra were fitted using a Visual Basic macro in Microsoft Excel.[17] The fitted spectra are shown in the Supporting Information as Figure S-2, and a summary of the parameters recovered from the fitting is provided in Table 1.

Several interesting features emerge from Table 1 with respect to the parameters recovered from the spectral fits. First, while the 0−0 emission energy (E_{00}) for $(\mathbf{PtC_8})_1$ is ca. 350 cm^{-1} higher than that for $(\mathbf{PtC_8})_2$, the energy difference between $(\mathbf{PtC_8})_2$ and $(\mathbf{PtC_8})_3$ is only ca. 30 cm^{-1}. Second, the Huang−Rhys parameter (S_m) decreases substantially from $(\mathbf{PtC_8})_1$ to $(\mathbf{PtC_8})_2$; however. it does not change significantly from the latter to $(\mathbf{PtC_8})_3$. Both features indicate that the triplet exciton delocalization is within approximately two PtC_8 repeat units.

Transient Absorption Spectroscopy. To provide additional information regarding the properties of the triplet state of the oligomers, nanosecond transient absorption spectra were recorded at room temperature in deoxygenated THF solution. As shown in Figure 4, all three structures feature strong triplet−

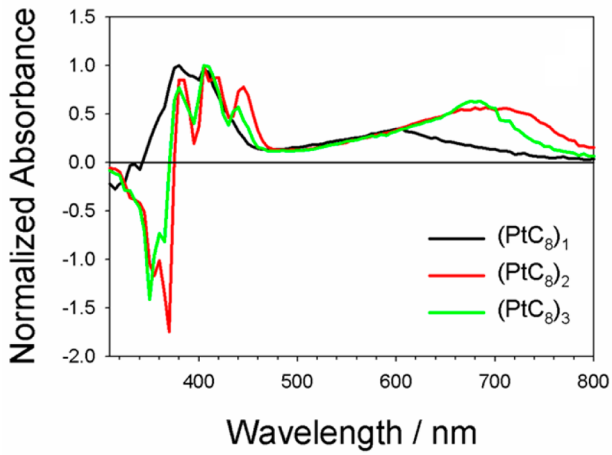

Figure 4. Normalized transient absorption spectra of $(\mathbf{PtC_8})_n$ at t = 0 μs. Spectra obtained from global analysis of time-resolved multi-wavelength difference absorption spectra.

triplet absorption in the visible region combined with bleaching of the ground-state absorption bands in the near-UV (also see Figure S-3 in the Supporting Information for triplet absorption difference spectra at various delay times). Interestingly, the triplet absorption for each oligomer consists of two distinct bands: the first more intense band that appears at short wavelengths (370−450 nm) and a second relatively weaker band that appears at longer wavelength in the red- to near-infrared region. The short wavelength bands appear to have a vibrational structure (especially evident in $(\mathbf{PtC_8})_2$ and $(\mathbf{PtC_8})_3$). However, a clear assignment of the structure to vibronic coupling is complicated due to overlap of the excited-state absorption with the ground-state bleach, which itself features a pronounced vibronic progression. Interestingly, the shape and position of the low energy triplet−triplet absorption band varies across the oligomer series (see Figure 4), suggesting the triplet absorption accesses a level that is delocalized across the entire oligomer structure. Lifetimes recovered from

Table 1. Emission Spectra Fitting Parameters for $(\mathbf{PtC_8})_n$ Complexes at 100 K

	$\lambda_{max,em}$/nm	E_{00}/cm^{-1}	$\hbar\omega$/cm^{-1}	$\Delta\nu_{0,1/2}$/cm^{-1}	S_m	ΔE_{ST}/eV
$(PtC_8)_1$	584	17 123	2100	230	0.9	0.64
$(PtC_8)_2$	595	16 778	2045	250	0.5	0.50
$(PtC_8)_3$	595	16 806	2085	235	0.4	0.50

transient absorption spectra are on a time scale of a few hundred nanoseconds and increase with the oligomer chain length. (The decay profiles are shown in Figure S-4 in the Supporting Information and lifetimes are shown in Table 2.) Furthermore, although triplet yields (Φ_{isc}) were not determined, the fact that the triplet−triplet absorptions are relatively intense (the typical ΔA_{max} values are >0.1; see Figure S-3 in the Supporting Information) and the lack of fluorescence strongly suggests that $\Phi_{isc} \approx 1$ for the oligomers.

To gain insight regarding the electronic basis of the triplet−triplet absorption spectra, electronic structure calculations were carried out on $(\mathbf{PtC_8})_1'$ to $(\mathbf{PtC_8})_2'$ using time-dependent density functional theory (TD-DFT). Tables S-1 and S-2 in the Supporting Information summarize the results of these calculations for $(\mathbf{PtC_8})_1'$ and $(\mathbf{PtC_8})_2'$. Careful consideration of the TD-DFT results for the triplet states reveals that the high-energy triplet−triplet absorption (390−400 nm) has contributions from transitions involving orbitals that are located at energies close to the HOMO and LUMO of the ground state (Table S-2 in the Supporting Information); for example, for $(\mathbf{PtC_8})_2'$ this is LSOMO (218α) → LUMO+1 (220α). This explains why the high-energy triplet−triplet transition is energetically close to the low-energy singlet-ground state absorption, which for $(\mathbf{PtC_8})_2'$ is dominated by the HOMO−LUMO transition (218 → 219, Table S-1 in the Supporting Information). By contrast, for the low energy triplet−triplet absorption band, the transitions involve excitation of the unpaired electrons to levels that are in relatively closer energetic proximity (e.g., they are analogous to "mid-gap" transitions in doped conjugated polymers)[23] Specifically, for $(\mathbf{PtC_8})_2'$ the calculations show that the low-energy band has substantial contributions from HOMO−2 (216β) → LSOMO (218β) and HSOMO (219α) → LUMO+2 (211α), where the latter transition involves excitation of the excited electron into a unfilled orbital, which is relatively close in energy to the LUMO of the ground state. Additionally, the computations show that the low-energy transitions are strongly delocalized for both $(\mathbf{PtC_8})_1'$ and $(\mathbf{PtC_8})_2'$, confirming the sensitivity of the electronic transitions to oligomer length. While the HSOMO of $(\mathbf{PtC_8})_2'$ is localized to one repeat unit, the LSOMO is mostly delocalized.

Phosphorescence Decay Kinetics. To gain insight concerning the temperature dependence of the triplet lifetimes for the $(\mathbf{PtC_8})_n$ series, time-resolved emission studies were carried out in deoxygenated Me-THF solution (glass) over the 100−300 K temperature range. The lifetimes recovered from time-resolved emission by spectral decay fitting are plotted as a function of temperature, as shown in Figure 5. Several interesting features emerge from Figure 5. First, for all three oligomers, the emission lifetimes decrease with increasing temperature. In particular, the lifetimes decrease slightly more rapidly in the temperature region corresponding to the glass-to-fluid transition of Me-THF (120−140 K). Second, the emission lifetimes increase with oligomer chain length in the whole temperature region.

The radiative and nonradiative decay rates (k_r and k_{nr}) of the triplet state can be calculated using eqs 4 and 5, which are obtained by rearrangement of eqs 2 and 3.

$$\tau_T = \frac{1}{k_r + k_{nr}} \tag{2}$$

$$\Phi_p = \Phi_{isc} k_r \tau_T \tag{3}$$

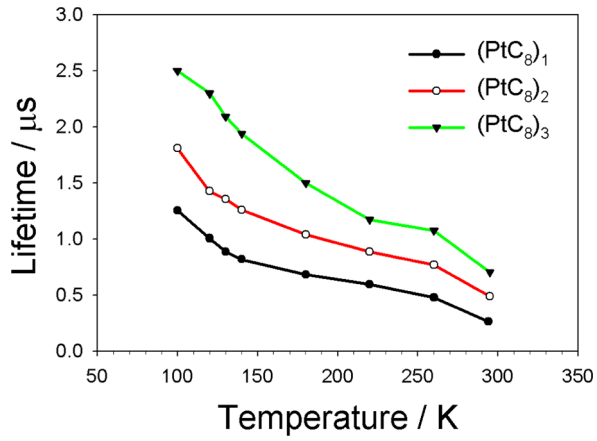

Figure 5. Temperature dependence of photoluminescence lifetimes for $(\mathbf{PtC_8})_n$ in deoxygenated Me-THF solution (glass).

$$k_{nr} = \left[1 - \left(\frac{\Phi_p}{\Phi_{isc}}\right)\right]\frac{1}{\tau_T} \tag{4}$$

$$k_r = \left(\frac{\Phi_p}{\Phi_{isc}}\right)\frac{1}{\tau_T} \tag{5}$$

In these expressions τ_T is the triplet lifetime, Φ_p is phosphorescence quantum yield, and Φ_{isc} is intersystem crossing efficiency. The values of τ_T, Φ_p, and Φ_{isc} are needed to compute k_r and k_{nr}. Here τ_T and Φ_p are known and Φ_{isc} is unknown. However, as previously noted, we believe that the intersystem crossing efficiency (Φ_{isc}) is close to unity ($\Phi_{isc} \approx 1$). Furthermore, because Φ_p is small, $\Phi_p \ll \Phi_{isc}$, and under these conditions eqs 4 and 5 can be further simplified to afford eqs 6 and 7.

$$k_{nr} \approx \frac{1}{\tau_T} \tag{6}$$

$$k_r \approx \frac{\Phi_p}{\tau_T} \tag{7}$$

The values of k_r and k_{nr} computed from the experimental data are listed in Table 2, and several features are worth noting with respect to these data. First, for all three oligomers, the values of k_{nr} exceed k_r by about 1000-fold, indicating that nonradiative decay is the dominant decay path for the oligomers. Second, the radiative rate is relatively constant for the series at $\sim 5 \times 10^3$ s^{-1}. This finding is similar to the results seen in our previous study of the Pt-capped carbon chains (Scheme 1).[17] Third and most interesting is the fact that the nonradiative decay rate systematically decreases with increasing oligomer length. (Note that this trend is clear in the fact that the phosphorescence and transient absorption lifetimes increase with oligomer length.)

Structure and Delocalization of the Triplet Exciton in Carbon-Chain Oligomers. As noted in the Introduction, we previously examined the spectroscopy and dynamics in a series of Pt-capped oligoynes (Scheme 1, $\mathbf{Pt_2}(C)_n$).[17] On the basis of the evolution of the triplet energy and nonradiative decay rates within this series it was concluded that the triplet is delocalized over ≥12 carbon atoms, corresponding to a segment consisting of at least a hexayne segment (−(C≡C)$_6$−). In the present study, we sought to determine how "oligomerization" of a

Table 2. Photophysical Parameters for the Complexes $(PtC_8)_n$

	$\tau_T/10^{-6}$ s[a]	Φ_p[a]	$k_{nr}/10^6$ s^{-1}[a]	$k_r/10^3$ s^{-1}[a]	$\tau_T/10^{-6}$ s[b]	$k_{nr}/10^5$s[b]	τ/μs[c]
$(PtC_8)_1$	0.26	0.0011	3.8	4.1	1.25	8.0	0.22
$(PtC_8)_2$	0.49	0.0025	2.1	5.1	1.81	5.5	0.45
$(PtC_8)_3$	0.70	0.0031	1.4	4.4	2.50	4.0	0.62

[a]Phosphorescence decay measured at room temperature. [b]Measured at 100 K. [c]Extracted from room temperature transient absorption.

tetrayne (C_8) segment influences the energy and dynamics of the triplet exciton. In the present study, information regarding the triplet state comes from several observables: (1) absorption spectroscopy; (2) phosphorescence spectroscopy and decay dynamics; and 3) triplet−triplet absorption spectroscopy. The results of these experiments paint a consistent picture of the triplet state in the oligomer systems. First, the absorption and phosphorescence spectroscopy reveal that the $S_o \rightarrow S_1$ and $T_1 \rightarrow S_o$ transitions shift to lower energy from $(\mathbf{PtC_8})_1$ to $(\mathbf{PtC_8})_2$ but then remain approximately the same for $(\mathbf{PtC_8})_3$. Comparing the results from the present study with those for the $\mathbf{Pt_2(C_2)}_n$ oligomers previously studied (Scheme 1) shows that the triplet energy for $(\mathbf{PtC_8})_1$ is approximately the same as that for $\mathbf{Pt_2(C_2)_4}$. However, the triplet energy of $(\mathbf{PtC_8})_2$ and $(\mathbf{PtC_8})_3$ is somewhat larger compared with that of $\mathbf{Pt_2(C_2)_5}$. This reveals that the effect of C_8 "dimerization" on the triplet energy is less than occurs by the simple addition of two more carbons in the chain (e.g., $\mathbf{Pt_2(C_2)_4} \rightarrow \mathbf{Pt_2(C_2)_5}$). These findings are in accord with previous studies of platinum-acetylide chromophores, which generally reveal that the triplet excited state is not substantially delocalized through intervening Pt(II)-centers that link π-electron systems.[1,24−27]

While the absorption and emission spectroscopic results point to a relatively localized triplet state, there are subtle hints that the triplet exciton structure and dynamics are affected, either directly or indirectly, by oligomerization of the C_8 chains in $(\mathbf{PtC_8})_2$ and $(\mathbf{PtC_8})_3$. Thus, the emission spectral fitting shows that the Huang−Rhys parameter, S_m, decreases slightly between $n = 2$ and 3. In addition, the nonradiative decay rate also decreases continuously across the entire series. These results point to the fact that the triplet is further delocalized by the increased chain length in $n = 3$ compared with $n = 2$. An interesting possibility is that these affects arise due to a dynamic "hopping" of a more localized triplet exciton between C_8 chains, for example, as suggested by the following equation for $(\mathbf{PtC_8})_3$:

$$\text{Cl-}^3[\text{PtP}_2\text{-(C}\equiv\text{C)}_4\text{-PtP}_2]^*\text{-(C}\equiv\text{C)}_4\text{-PtP}_2\text{-(C}\equiv\text{C)}_4\text{-PtP}_2\text{-Cl} \leftrightarrows$$
$$\text{Cl-PtP}_2\text{-(C}\equiv\text{C)}_4\text{-}^3[\text{PtP}_2\text{-(C}\equiv\text{C)}_4\text{-PtP}_2]^*\text{-(C}\equiv\text{C)}_4\text{-PtP}_2\text{-Cl} \leftrightarrows$$
$$\text{Cl-PtP}_2\text{-(C}\equiv\text{C)}_4\text{-PtP}_2\text{-(C}\equiv\text{C)}_4\text{-}^3[\text{PtP}_2\text{-(C}\equiv\text{C)}_4\text{-PtP}_2]^*\text{-Cl} \quad (8)$$

Similar dynamic triplet hopping was probed in a series of monodisperse oligomers of the type, *all-trans*-$[PtP_2-(C\equiv C-C_6H_4-C\equiv C)]_n-$, where C_6H_4 is1,4-phenylene, and the unit to unit triplet hopping was found to occur with a time constant ∼25 ps.[18] While it is not possible to distinguish whether such a triplet hopping process in $(\mathbf{PtC_8})_2$ and $(\mathbf{PtC_8})_3$ happens, future experiments using time-resolved infrared spectroscopy[28] could provide insight into the structure and dynamics of triplet exciton hopping in this and related structures.

■ SUMMARY AND CONCLUSIONS

A detailed photophysical investigation of a series of platinum tetrayne oligomers has been carried out. The photophysics of these oligomers is dominated by a $^3\pi,\pi^*$ state that is concentrated on the $-(C\equiv C)_4-$ chain. The low-temperature emission spectrum of each oligomer shows an intense and narrow phosphorescence band followed by a vibronic progression of sub-bands separated by ca. 2100 cm^{-1} that responds to the stretch of the $-(C\equiv C)_4-$ chain. Both absorption and emission bands are red-shifted ∼10 nm (650 and 290 cm^{-1}, respectively) from $(\mathbf{PtC_8})_1$ (λ_{abs} = 388 nm ; λ_{em} = 585 nm)to $(\mathbf{PtC_8})_2$ (λ_{abs} = 398 nm; λ_{em} = 595 nm) and then shifted a little from $(\mathbf{PtC_8})_2$ to $(\mathbf{PtC_8})_3$, suggesting that the triplet exciton is delocalized over at most two repeat units. Room-temperature transient absorption measurements also support the notion of triplet delocalization, even suggesting that there is increased delocalization in $(\mathbf{PtC_8})_3$.

The platinum centers in the carbon chain oligomers play several roles beyond serving to link together the C_8 chains. First, $d\pi$(Pt)−$p\pi$(C) overlap allows electronic interaction between two C_8 chains. This interaction leads to delocalization in the singlet state and to a lesser extent in the triplet state. Second, the Pt centers introduce strong spin−orbit coupling, leading to very efficient singlet → triplet intersystem crossing as well as the observation of phosphorescence, even at ambient temperature in fluid solution. The latter effect allows facile study of the triplet state in these remarkable linear carbon chain oligomers.

■ ASSOCIATED CONTENT

Supporting Information

Excitation spectra and fitted phosphorescence emission spectra of platinum tetrayne oligomers. Results of time-dependent density functional theory calculations. This material is available free of charge via the Internet at http://pubs.acs.org.

■ AUTHOR INFORMATION

Corresponding Authors

*E-mail: gladysz@mail.chem.tamu.edu (J.A.G).
*E-mail: kschanze@chem.ufl.edu (K.S.S.).

Notes

The authors declare no competing financial interest.

■ ACKNOWLEDGMENTS

This work was supported by the National Science Foundation (grant no. CHE-115164 (K.S.S.) and grant no. CHE-1153085 (J.A.G.)). We acknowledge the University of Florida Research Computing for providing computational resources and support that contributed to the research results reported in this publication (http://researchcomputing.ufl.edu).

■ REFERENCES

(1) Glusac, K.; Kose, M. E.; Jiang, H.; Schanze, K. S. Triplet Excited State in Platinum-Acetylide Oligomers: Triplet Localization and Effects of Conformation. *J. Phys. Chem. B* **2007**, *111*, 929−940.

(2) Eisler, S.; Slepkov, A. D.; Elliott, E.; Luu, T.; McDonald, R.; Hegmann, F. A.; Tykwinski, R. R. Polyynes as a Model for Carbyne: Synthesis, Physical Properties, and Nonlinear Optical Response. *J. Am. Chem. Soc.* **2005**, *127*, 2666−2676.

(3) Dembinski, R.; Bartik, T.; Bartik, B.; Jaeger, M.; Gladysz, J. A. Toward Metal-Capped One-Dimensional Carbon Allotropes: Wirelike C6-C20 Polyynediyl Chains That Span Two Redox-Active (η_5-C_5Me_5)Re(NO)(PPh_3) Endgroups. *J. Am. Chem. Soc.* **2000**, *122*, 810−822.

(4) Szafert, S.; Gladysz, J. A. Carbon in One Dimension: Structural Analysis of the Higher Conjugated Polyynes. *Chem. Rev.* **2003**, *103*, 4175−4205.

(5) Gibtner, T.; Hampel, F.; Gisselbrecht, J.-P.; Hirsch, A. End-Cap Stabilized Oligoynes: Model Compounds for the Linear sp Carbon Allotrope Carbyne. *Chem.—Eur. J.* **2002**, *8*, 408−432.

(6) Meyer, W. E.; Amoroso, A. J.; Horn, C. R.; Jaeger, M.; Gladysz, J. A. Synthesis and Oxidation of Dirhenium C_4, C_6, and C_8 Complexes of the Formula (η5-C_5Me_5)Re(NO)(PR_3)$(CC)_n$(R_3P)(ON)Re(η_5-C_5Me_5) (R = 4-C_6H_4R', c-C_6H_{11}): In Search of Dications and Radical Cations with Enhanced Stabilities. *Organometallics* **2001**, *20*, 1115−1127.

(7) Yam, V. W.-W. Luminescent Carbon-Rich Rhenium(I) Complexes. *Chem. Commun.* **2001**, 789−796.

(8) Che, C.-M.; Chao, H.-Y.; Miskowski, V. M.; Li, Y.; Cheung, K.-K. Luminescent μ-Ethynediyl and μ-Butadiynediyl Binuclear Gold(I) Complexes: Observation of $^3(\pi,\pi^*)$ Emissions from Bridging C_n^{2-} Units. *J. Am. Chem. Soc.* **2001**, *123*, 4985−4991.

(9) Chalifoux, W. A.; McDonald, R.; Ferguson, M. J.; Tykwinski, R. R. *tert*-Butyl-End-Capped Polyynes: Crystallographic Evidence of Reduced Bond-Length Alternation. *Angew. Chem., Int. Ed.* **2009**, *48*, 7915−7919.

(10) Samoc, M.; Dalton, G. T.; Gladysz, J. A.; Zheng, Q.; Velkov, Y.; Agren, H.; Norman, P.; Humphrey, M. G. Cubic Nonlinear Optical Properties of Platinum-Terminated Polyynediyl Chains. *Inorg. Chem.* **2008**, *47*, 9946−9957.

(11) Adams, D. M.; Brus, L.; Chidsey, C. E. D.; Creager, S.; Creutz, C.; Kagan, C. R.; Kamat, P. V.; Lieberman, M.; Lindsay, S.; Marcus, R. A.; Metzger, R. M.; Michel-Beyerle, M. E.; Miller, J. R.; Newton, M. D.; Rolison, D. R.; Sankey, O.; Schanze, K. S.; Yardley, J.; Zhu, X. Charge Transfer on the Nanoscale: Current Status. *J. Phys. Chem. B* **2003**, *107*, 6668−6697.

(12) Ballmann, S.; Hieringer, W.; Secker, D.; Zheng, Q. L.; Gladysz, J. A.; Gorling, A.; Weber, H. B. Molecular Wires in Single-Molecule Junctions: Charge Transport and Vibrational Excitations. *ChemPhysChem* **2010**, *11*, 2256−2260.

(13) Stahl, J.; Bohling, J. C.; Bauer, E. B.; Peters, T. B.; Mohr, W.; Martin-Alvarez, J. M.; Gladysz, J. A. sp Carbon Chains Surrounded by sp^3 Carbon Double Helices: A Class of Molecules That Are Accessible by Self-Assembly and Models for Insulated Molecular-Scale Devices. *Angew. Chem., Int. Ed.* **2002**, *41*, 1872−1876.

(14) Bruce, M. I.; Low, P. J.; Costuas, K.; Halet, J.-F.; Best, S. P.; Heath, G. A. Oxidation Chemistry of Metal-Bonded C_4 Chains: A Combined Chemical, Spectroelectrochemical, and Computational Study. *J. Am. Chem. Soc.* **2000**, *122*, 1949−1962.

(15) Yam, V. W.-W.; Wong, K. M.-C.; Zhu, N. Luminescent Platinum(II) Terpyridyl-Capped Carbon-Rich Molecular Rods—an Extension from Molecular- to Nanometer-Scale Dimensions. *Angew. Chem., Int. Ed.* **2003**, *42*, 1400−1403.

(16) Mohr, W.; Stahl, J.; Hampel, F.; Gladysz, J. A. Synthesis, Structure, and Reactivity of sp Carbon Chains with Bis(Phosphine) Pentafluorophenylplatinum Endgroups: Butadiynediyl (C_4) through Hexadecaoctaynediyl (C_{16}) Bridges, and Beyond. *Chem.—Eur. J.* **2003**, *9*, 3324−3340.

(17) Farley, R. T.; Zheng, Q.; Gladysz, J. A.; Schanze, K. S. Photophysics of Diplatinum Polyynediyl Oligomers: Chain Length Dependence of the Triplet State in sp Carbon Chains. *Inorg. Chem.* **2008**, *47*, 2955−2963.

(18) Keller, J. M.; Glusac, K. D.; Danilov, E. O.; McIlroy, S.; Sreearuothai, P.; Cook, A. R.; Jiang, H.; Miller, J. R.; Schanze, K. S. Negative Polaron and Triplet Exciton Diffusion in Organometallic "Molecular Wires". *J. Am. Chem. Soc.* **2011**, *133*, 11289−11298.

(19) Zheng, Q.; Hampel, F.; Gladysz, J. A. Longitudinally Extended Molecular Wires Based Upon Ptctcctcctcctc Repeat Units: Iterative Syntheses of Functionalized Linear PtC_8Pt, PtC_8PtC_8Pt, and $PtC_8PtC_8PtC_8Pt$ Assemblies. *Organometallics* **2004**, *23*, 5896−5899.

(20) Stultz, L. K.; Binstead, R. A.; Reynolds, M. S.; Meyer, T. J. Epoxidation of Olefins by $[Ru^{IV}(bpy)_2(py)(O)]^{2+}$ in Acetonitrile Solution. A Global Kinetic Analysis of the Epoxidation of Trans-Stilbene. *J. Am. Chem. Soc.* **1995**, *117*, 2520−2532.

(21) Nagano, Y.; Ikoma, T.; Akiyama, K.; Tero-Kubota, S. Symmetry Switching of the Fluorescent Excited State in Diphenylpolyynes. *J. Am. Chem. Soc.* **2003**, *125*, 14103−14112.

(22) Whittle, C. E.; Weinstein, J. A.; George, M. W.; Schanze, K. S. Photophysics of Diimine Platinum(II) bis-Acetylide Complexes. *Inorg. Chem.* **2001**, *40*, 4053−4062.

(23) Patil, A. O.; Heeger, A. J.; Wudl, F. Optical-Properties of Conducting Polymers. *Chem. Rev.* **1988**, *88*, 183−200.

(24) Liu, Y.; Jiang, S.; Glusac, K.; Powell, D. H.; Anderson, D. F.; Schanze, K. S. Photophysics of Monodisperse Platinum-Acetylide Oligomers: Delocalization in the Singlet and Triplet Excited States. *J. Am. Chem. Soc.* **2002**, *124*, 12412−12413.

(25) Beljonne, D.; Wittmann, H. F.; Kohler, A.; Graham, S.; Younus, M.; Lewis, J.; Raithby, P. R.; Khan, M. S.; Friend, R. H.; Bredas, J. L. Spatial Extent of the Singlet and Triplet Excitons in Transition Metalcontaining Poly-ynes. *J. Chem. Phys.* **1996**, *105*, 3868−3877.

(26) Rogers, J. E.; Cooper, T. M.; Fleitz, P. A.; Glass, D. J.; McLean, D. G. Photophysical Characterization of a Series of Platinum(II)-Containing Phenyl-Ethynyl Oligomers. *J. Phys. Chem. A* **2002**, *106*, 10108−10115.

(27) Cooper, T. M.; Krein, D. M.; Burke, A. R.; McLean, D. G.; Rogers, J. E.; Slagle, J. E. Asymmetry in Platinum Acetylide Complexes: Confinement of the Triplet Exciton to the Lowest Energy Ligand. *J. Phys. Chem. A* **2006**, *110*, 13370−13378.

(28) Chisholm, M. H.; Gustafson, T. L.; Turro, C. Photophysical Properties of Mm Quadruply Bonded Complexes Supported by Carboxylate Ligands, MM = Mo_2, MoW, or W_2. *Acc. Chem. Res.* **2012**, *46*, 529−538.